

INTENSITY CALIBRATION AND IMAGING WITH SWISSRANGER SR-3000 RANGE CAMERA

A. Jaakkola^{*}, S. Kaasalainen, J. Hyyppä, H. Niittymäki, A. Akujärvi

Department of Remote Sensing and Photogrammetry, Finnish Geodetic Institute, 02431 Masala, Finland –
(anttoni.jaakkola, sanna.kaasalainen, juha.hyyppa, henri.niittymaki, altti.akujarvi)@fgi.fi

Commission III, WG III/3

KEY WORDS: Calibration, Infrared, Image, Camera, LIDAR, Radiometry, Close Range.

ABSTRACT

Intensity images acquired with range imaging instruments can be used in the future for various applications, e.g. face recognition, assisting blind people in travelling and walking, automatic robotic vision, rendering 3D models and improving automatic recognition of objects. For the intensity information to be usable, it needs to be radiometrically calibrated. In this paper we propose the first empirical radiometric calibration method for range cameras to reduce errors caused by distance from the target and illumination falloff. With the proposed method we are able to correct images and facilitate their further use as well as make reflectance measurements. The use of range cameras in remote sensing is a new field of study, and no radiometric calibration methods for the intensity have thus far been proposed. We show that intensity calibration of the range camera is possible and applicable in remote sensing.

1. INTRODUCTION

1.1 Background

Calibration and use of intensity images from range imaging instruments such as range cameras and laser scanners is a new field of study. Some work on radiometric calibration of intensity images has been done in the field of airborne (Wagner, 2006; Ahokas, 2006; Kaasalainen, 2007a) and terrestrial laser scanning (Kaasalainen, 2007b). However, miniature 3D imaging cameras have just recently entered the market, and range imaging has now become an object of technical and scientific interest (see Blanc (2004) and Oggier et al. (2005) for a summary and review). Kahlmann et al. (2006) have studied the calibration of the range measurement and achieved results in the centimetre range, but to our knowledge, no work has been published on intensity measurements and calibration of 3D range cameras. In this paper, we propose a new method and present the first results of an empirical intensity calibration method for a miniature 3D range camera.

The need to develop an intensity calibration method for range cameras is apparent. Range cameras are powerful tools for close-range 3D imaging at fast speed (3D video), and automatic processing tools are needed before we can benefit from these instruments to their full extent. By calibrating intensity values recorded by the 3D camera, automatic classification and recognition tools can be developed. Application areas where we expect significant benefits include

- automatic classification of objects (such as trees, roads, buildings, and people) to be used in robotic vision, obstacle mapping for blind people, and mapping of vehicle surroundings
- automatic face recognition

- mobile mapping (automatic mapping of road environment)
- personal mapping
- rendering 3D models
- industrial quality analysis

There is a need to calibrate the intensity, since wide scale of ranges is used in close-range measurements and the range effect corrupts the intensity.

1.2 Distance and Intensity Correction

Thus far most of the work on intensity calibration for laser scanning (Wagner, 2006; Ahokas, 2006) has been based on the radar equation, as it provides intensity values that are not dependent on the measurement range

$$P_r = \frac{P_t G_t A_r \sigma F^4}{(4\pi)^2 R_t^2 R_r^2} \quad (1)$$

where P_r is received power, P_t transmitted power, G_t gain of the transmitting antenna, A_r effective aperture of the receiving antenna, σ radar cross section, F pattern propagation factor, R_t distance from the transmitter to the target and R_r distance from the target to the receiver. Equation 1 was also the starting point of our research. By assuming that all variables except distance from the target remain constant and that the target fills the whole area of a pixel, which leads to σ being proportional to R^2 , we can reduce the equation to

^{*} Corresponding author

$$P_r = \frac{K}{R^2} \quad (2)$$

where K is a constant combining all the coefficients (P_t , G_r , A_r , σ and F) and R is the distance between the camera and the target.

In addition to the distance correction of the image, the effect of vignetting must also be reduced in the images. In traditional photogrammetry, this is often approximated by the \cos^4 law of illumination falloff, which can be broken down into

$$\cos(\alpha)\cos^3(\beta) \quad (3)$$

where α is the angle from the optical axis in object space and β is the corresponding angle in image space. This is not an exact physical model of the intensity distribution over the image, partly because the illumination is not uniform, but it has proven in practice to model most of the intensity falloff (cf. Slater 1980, pp. 116-119).

In this paper, we propose a method for calibrating the reflectance measurement of the SwissRanger SR-3000 range camera. We first eliminate the errors caused by distance from the target. Then we move on to the errors in the intensity measurement and finally we examine the results from the laboratory environment and the effect on real life images. The experiments are described in Sect. 2. The calibration procedures for range and image correction are presented in Sect. 3, and the results and conclusion in Sect. 4 and 5, respectively.

2. TEST SETUP

The SwissRanger SR-3000 made by CSEM (currently Mesa Imaging) is a phase shift based range camera with a non-ambiguity range of 7.5 m, a focal length of 8 mm, and pixel pitch of 40 mm. The illumination module consists of 55 NIR LEDs with a 850 nm wavelength and a total illumination power of less than 1 W. The range is measured from the phase shift of the 20 MHz signal, modulated into the illumination. The intensity image acquired by the camera is produced from the amplitude information of the reflected signal, and therefore the intensity value should be independent of the light coming from the environment. (Oggier et al., 2005)

For the modelling and calibration of the intensity measurements, we made two sets of measurements. One set was acquired by taking images of a silver screen with distances ranging from 0.55 to 3.95 meters with 0.1 m spacing. In the second set, the distances between the camera and the target varied from 0.5 m to 3.9 m (in 0.1 m increments). The target was a Spectralon® (Labsphere Inc.) reference plate of four stripes with different nominal reflectances: 99%, 50%, 25% and 12%. The manufacturer calibrated the Spectralon plate, and the respective calibrated values at 850 nm are 0.988, 0.523, 0.254 and 0.142. The test setups are depicted in Figure 1. To produce a reference distance scale, the distance of the camera and the target was measured for both sets using a standard measure tape.

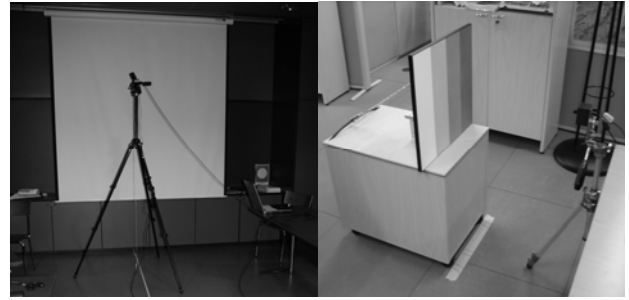


Figure 1. Test setups: measurement of the silver screen (left) and the 4-step Spectralon reference panel (right).

Raw intensity measurements from the Spectralon test are shown in Figure 2.

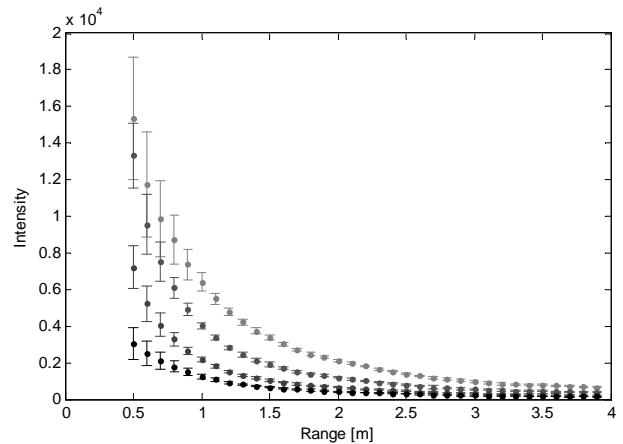


Figure 2. Raw intensity measurements from the second test showing the measured intensities for 99% (light grey), 50% (grey), 25% (dark grey) and 12% (black) Spectralon stripes.

To assess the applicability of the calibration method in some of the possible applications, images of outdoor targets were taken both with and without Spectralon reference targets.

3. CALIBRATION METHOD

3.1 Range Calibration and Correction

Because the intensity measurement is relative to the inverse square of the distance, accuracy of the range measurements is crucial. The original range measurements from the camera had an offset of ca. 0.2 m, and there was a sinusoidal error with amplitude of a few centimetres. We approximated the range measurement with an empirical sinusoidal function

$$R = a_2 \sin(\alpha R_0 + \beta) + a_1 R_0 + a_0 \quad (4)$$

where a_2 , a_1 , a_0 , α and β are coefficients fitted by the least squares method, R is the actual distance measured with a measuring tape, and R_0 is the distance measured by the camera. Figure 3 shows the errors of the original range measurements and the corrected ranges.

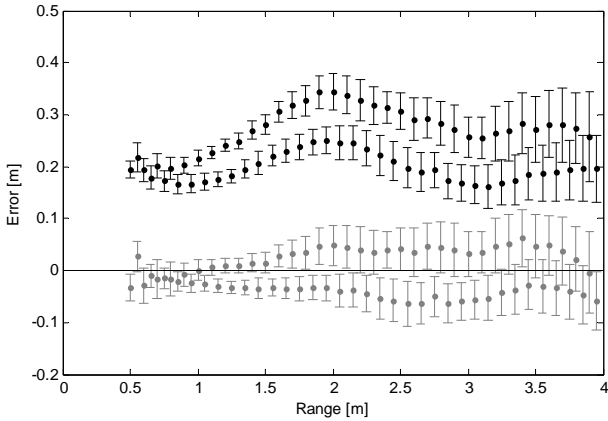


Figure 3. Distance offsets before and after applying the correction. Black dots represent the measurements from the camera and grey dots are corrected measurements relative to the tape measurement made during the experiment.

As we can see in Figure 3 most of the corrected measurements fall within 5 cm of the ground truth even though there is some deviation. The offset between the two datasets is probably caused by measurement errors in the reference measurements and the test setup. It would be possible to get better range corrections using the calibration method proposed by Kahlmann et al. (2006), but since our main objective was to study the calibration of intensity rather than the range, we decided not to do such extensive range calibration and instead used the simple empirical model described above. After range calibration, the measured intensities were corrected for range using the reduced radar equation (2).

3.2 Image Uniformity Calibration

Vignetting causes the intensity measured by the camera to fall as the angle from the optical axis increases. This effect can be modelled with the \cos^4 law, which incorporates the physical, optical and geometrical phenomena that cause illumination falloff (Slater 1980). The β value calculated from the camera specifications did not seem to model the falloff accurately enough, so we decided to use 2β as the angle, which seemed to fit much better.

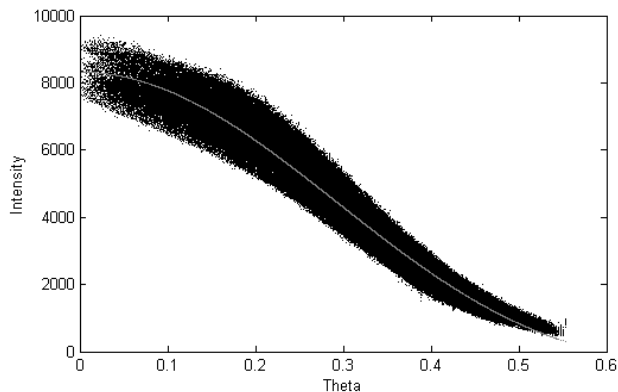


Figure 4. Illumination falloff and the \cos^4 curve (grey) fitted to the silver screen measurements (black) with ranges from 1.0 m to 1.7 m.

We do not have physical explanation why 2β behaves better than β but the empirical results support our decision. It may be due to some effects caused either by the camera optics or image pre-processing that is different from those in the traditional photogrammetric cameras. Also the \cos^4 model does not take into account any of the irregularities caused by the uneven illumination. The falloff of the range-corrected intensities and the \cos^4 curve obtained with the least squares fit are shown in Figure 4.

3.3 Offset Removal

After distance and illumination falloff corrections we find that there are still some errors in the relative intensities as shown in Figure 5.

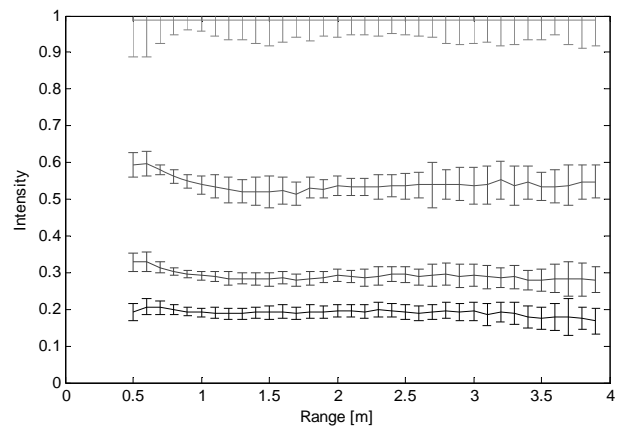


Figure 5. Intensities corrected for range and illumination falloff of the 4-step Spectralon panel scaled with 99% Spectralon (light grey) from the second experiment: 50% (grey), 25% (dark grey) and 12% (black).

We can see that the intensity values of the lower reflectance panels were too high. If we assume that this was caused by an offset in the raw intensity measurement we can approximate the offset by finding such a value that minimizes the standard deviation of corrected intensities for distance range from 1.0 m to 3.9 m. The shorter distances were omitted because of large relative errors.

After removing the offset, we found that the lower range and offset corrected reflectances were still relatively too high, which could be caused by an error in the range correction or a yet unknown base current or offset. This effect can be reduced by empirically finding such an offset for the range and offset-corrected intensities that the mean of the measurements equals the mean of the reference plates. After finding it, the offset can be removed from the measurements.

4. RESULTS

4.1 Image correction

Figure 6 shows both original and corrected intensity images. It provides a good illustration of the impact the calibration method has on image correction. The qualitative results of the proposed correction method are promising: we can effectively

remove the unevenness of the illumination and reduce fading of illumination over distance.

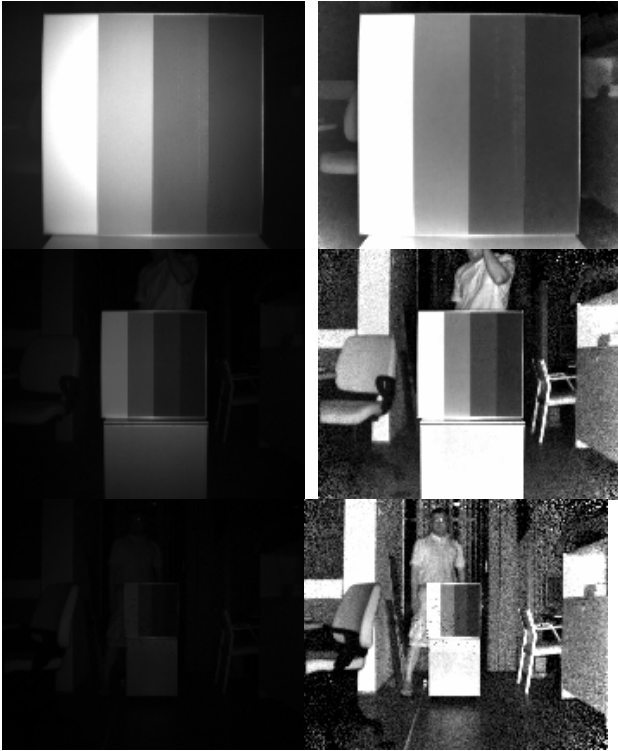


Figure 6. Images on the left are original images taken from a distance of 0.7 m, 1.5 m, and 3.0 m scaled to the mean of 99 % Spectralon measured from 0.7 m. Images on the right have been corrected with the presented method.

The uncorrected images in Figure 6 fade significantly over distance; the corrected images do not. The radial illumination falloff is also much lower in the corrected images than in the original images. Longer distances and peripheral regions of the image show high levels of noise in the corrected images because the integration time was kept constant for all the measurements. This could be partially avoided by adapting the integration time according to the measurement distance.

Images taken outdoors show that the method provides good results even in outdoor conditions where the solar illumination is likely to cause more noise. Figure 7 shows some examples of outdoor images before and after correction. We can see that the objects that are farther away from the camera lighten up and the halo caused by the illumination vanishes. On the other hand, the walls in the top panels of Figure 7 turn black when the distance to the target is greater than 4 m. Our correction method should compensate for the distance, but because of the limited illumination power, the reflected energy is too low to achieve intensity and distance readings that are accurate enough for compensation. Increasing the integration time could alleviate this problem.

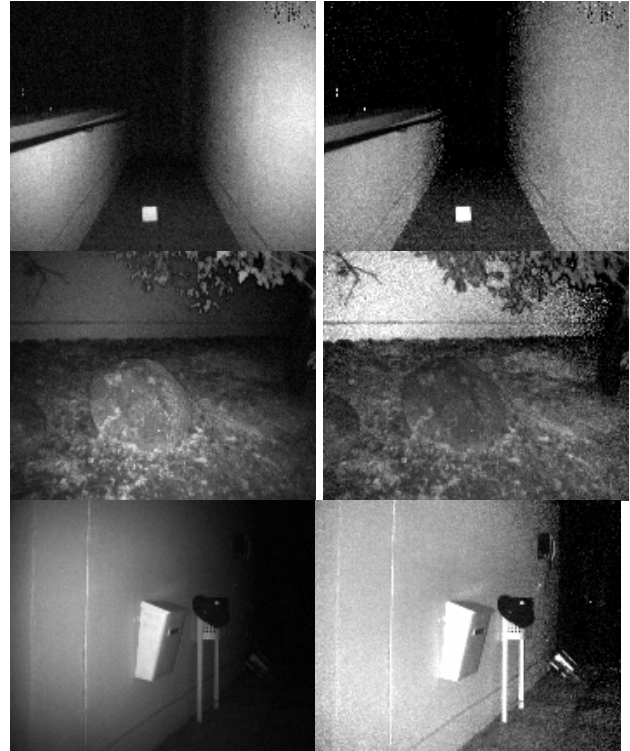


Figure 7. Outdoor pictures before and after correction. Images on the left are scaled to the maximum value of the image. Images on the right have been corrected with the presented method.

4.2 Reflectance measurements

After all corrections, i.e. range calibration, image uniformity correction and both intensity offsets, were applied, the results were those shown in figures 8 and 9.

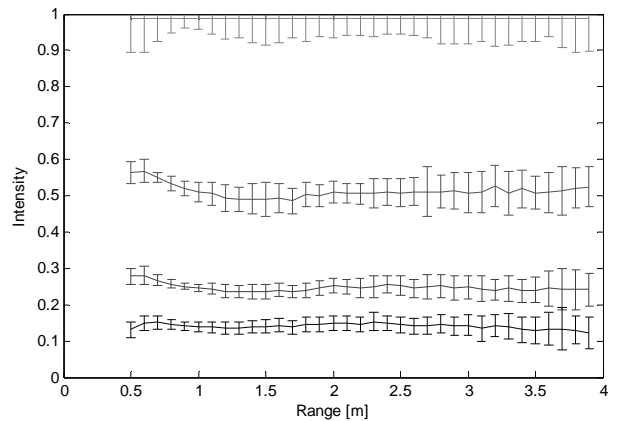


Figure 8. Intensities for 12% (black), 25% (dark grey), 50% (grey) and 99% (light grey) Spectralon panels scaled to the 99% Spectralon with standard deviations and with all corrections applied.

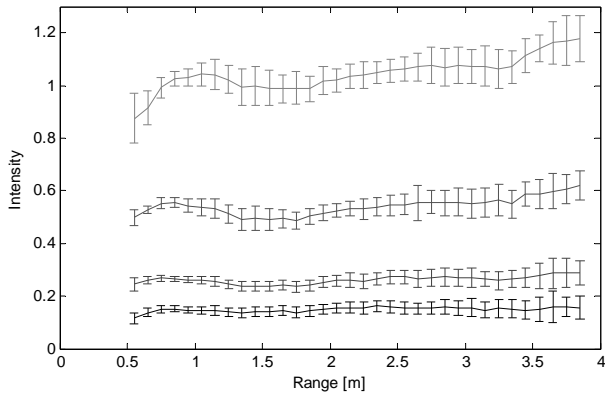


Figure 9. Corrected intensities for 12% (black), 25% (dark grey), 50% (grey) and 99% (light grey) Spectralons scaled to the silver screen measurements, i.e. the silver screen is assumed to have reflectance of 1.0.

As we can see in Figure 9, the intensity calibration with the silver screen can be applied to the Spectralon measurements. This suggests that the proposed calibration procedure is somewhat independent of the measurement conditions and also applicable in other environments. The relative reflectances had a standard deviation of 0.04 over the range of 1.0 m to 3.0 m and 0.06 over the whole measurement range.

Outdoor images taken to assess the results showed that the measurements are heavily dependent on the environment as opposed to the manufacturer's statement (Oggier, 2005). The 99% Spectralon plate placed into the target area in the top panel of Figure 7 shows a corrected reflectance of c. 1.4 relative to the silver screen, which implies that the background suppression is not perfect. Although the intensity value was measured from the amplitude of the reflected signal, the background illumination originating from the sun heavily distorted the measurement. Therefore, these quantitative results should only be applied in controlled environments, e.g. indoors.

5. CONCLUSION AND FUTURE WORK

The calibration method presented in this paper shows promising results. The effects of uneven illumination and the diminishing of the reflected power over distance were almost completely removed and the images became visually more appealing. Also the relative reflectances had a standard deviation of 0.06, and 70% of the measurements fell within 0.05 of the nominal reflectance. Scaling the measurements to the measurements of the silver screen showed that the method is also applicable in a wider range of environments than the one in which the calibration was made, as long as the background illumination does not become too dominant. The calibrated intensity measurements were consistent over the whole measurement range of distances.

Since this is a new type of instrument, all the error sources of the intensity measurements are not yet known, and therefore most of the corrections are based on empirical observations. Some of the errors are probably caused by the uneven illumination and phenomena in the optics that are not yet known. The offset seen in Figure 5 could be caused by errors in the range measurement.

Future work includes the implementation of physically-based models, improvement of the illumination falloff correction to better model the phenomenon, and improvement of the range calibration method by incorporating a more accurate distance measurement correction, such as the one proposed by Kahlmann (2006). One approach to improving radial correction would be to measure the evenness of the illumination originating from the camera's illumination module. The effect of integration time on the measurements should also be studied to enable accurate measurements over longer distances.

REFERENCES

- Ahokas, E., Kaasalainen, S., Hyyppä, J. & Suomalainen, J., 2006. Calibration of the Optech ALTM 3100 laser scanner intensity data using brightness targets. In: *International Archives of Photogrammetry, Remote Sensing and Spatial Information Sciences*, Marne-la-Vallee, France, Vol. XXXVI, Part 1A, CD-ROM.
- Blanc, N., Oggier, T., Gruener, G., Weingarten, J., Codourey, A. & Seitz, P., 2004. Miniaturized smart cameras for 3D-imaging in real-time. In: *Proc. IEEE Sensors 2004*, Vienna, Austria, Vol. 1, pp. 471-474.
- Kaasalainen, S., Hyyppä, J., Litkey, P., Hyyppä, H., Ahokas, E., Kukko, A. & Kaartinen, H., 2007a. Radiometric calibration of ALS intensity. In: *International Archives of Photogrammetry, Remote Sensing and Spatial Information Sciences*, Espoo, Finland, Vol. XXXVI, Part 3/W52, pp 201-205.
- Kaasalainen, S., Kukko, A., Lindroos, T., Litkey, P., Kaartinen, H., Hyyppä, J. & Ahokas, E., 2007b. Brightness measurements and calibration with airborne and terrestrial laser scanners. *IEEE Transactions on Geoscience and Remote Sensing*, Edinburgh, UK, Vol. 46(2), pp. 528-534.
- Kahlmann, T., Remondino, H. & Ingensand, H., 2006. Calibration for increased accuracy of the range imaging camera SwissRangerTM. In: *International Archives of Photogrammetry, Remote Sensing and Spatial Information Sciences*, Dresden, Vol. XXXVI, Part 5, pp. 136-141.
- Oggier, T., Büttgen, B., Lustenberger, F., Becker, G., Rüegg, B. & Hodac, A., 2005. SwissRanger SR3000 and first experiences based on miniaturized 3D-TOF cameras. In: *Proceedings of the 1st Range Imaging Research Day*. Zurich, Switzerland.
- Slater, P.N., 1980. *Remote sensing: optics and optical systems*, Addison-Wesley, 575 p.
- Wagner, W., Ullrich, A., Ducic, V., Melzer, T. & Studnicka, N., 2006. Gaussian decomposition and calibration of a novel small-footprint full-waveform digitizing airborne laser scanner. *ISPRS Journal of Photogrammetry and Remote Sensing*, Vol. 60(2), pp. 100-112.

ACKNOWLEDGMENT

This study was supported in part by the following Academy of Finland projects: Improving the Applicability of Intensity Information in Laser Scanning, The Use of ICT 3D Measurement Techniques for High-Quality Construction, and Transportation Data Acquisition by Means of ICT-Derived 3D Modelling.

